ON-SPECIMEN SENSORS FOR HIGH VELOCITY IMPACT TESTING OF HIGH-GRADE POLYMERS

J. P. Dear and J. H. MacGillivray *

This paper reports on a study of results obtained using sensors on polymers and similar materials for impact fracture toughness measurements. The different force-time and other data from sensors placed on different parts of the specimen are discussed and compared with those obtained from sensors on the striker. Mostly, this is for test conditions when strong transient forces are induced into the specimen that much contribute to its failure. These monitored strain data are related to information captured on high-speed photographic film as the specimen is taken to and beyond its failure point. Also, to optical and scanning electron-microscopic studies of the fracture surfaces.

INTRODUCTION

Many product designers are attracted to the increased toughness of new polymers that also have much improved dynamic properties generally. When evaluating these materials for their fracture resistance under high velocity impact, care is needed, in the location of strain gauges or other monitors, to obtain best data as to the forces acting on the crack initiation site and propagating the crack through the specimen. For lower impact velocities then sensors located in the striker and support points of a Charpy or similar tester may be all that is required to achieve faithful results. Whereas with high velocity tests then well-placed sensors on the specimen can also be needed. This is so as to obtain more reliable force-time and crack length measurements and process them to generate a variety of useful derived data such as critical stress intensity factor (K_c) and critical strain energy release rate (G_c) (Williams(1)). This is because the forces acting on the crack initiation site can differ from those acting on the specimen as a whole. The work presented in this paper is part of wider research into impact properties of materials employed in products of many different shapes and constructional features (Dear and MacGillivray (2)). This paper concentrates on three-point bend impact testing of high-density polyethylene (HDPE) materials.

* Department of Mechanical Engineering,
Imperial College of Science, Technology and Medicine,

EXPERIMENTAL

For this study, a drop-weight three-point bend impact tester was used with a falling mass of 65 kg. At a velocity of 5 m s^{-1} this gave an available energy of ca. 0.8 kJ to allow specimens to be tested of thickness B (12mm), width W (40mm) and overall length L (200mm), with a support span S (160mm) and a pre-notch of depth 15mm. At the root of the notch, a razor-sharp pre-crack of depth 5mm was made immediately before the test.The general arrangement is illustrated in Figure 1 which shows the specimen resting on two rollers of diameter 25mm and the impact striker having a tip radius of 10mm. A static load was used to calibrate the outputs from the strain gauges. The specimen was placed into the same calibration fixture in the two possible orientations to check sensitivity to slight misalignments. The on-specimen gauge was finally calibrated in the static test rig just prior to impact loading.

RESULTS

Figure 2 is a set of force-time test records obtained from fracturing a polyethylene (HDPE) specimen at room temperature at an impact velocity of 5 m s^{-1}. The force-time trace (a) was from the sensor embedded in the striker and traces (b) and (c) were those from two strain gauges attached to the specimen on one side of the crack. One was in a W/2xW/2 position and the other was in a W/2xW/8 position as illustrated in Figure 1. These were found to be the best positions for monitoring the forces acting on the crack tip and those in the compressed part of the specimen. Also for helping to determine the different failure rates for the fast crack in the core of the material, the tearing of the side-lips and the rupturing of the hinge bend material. This was achieved by comparing the W/2xW/2 and W/2xW/8 sensor outputs for specimens with and without side-grooves.The final phase of a specimen failure is the fracture of the hinge material. In some cases, the hinge can survive the impact and this results in additional kinetic energy being given to the fractured specimen as it is driven from its fixture. Shown with Figure 2 is an optical photograph of a fracture surface of a specimen without side-grooves which shows the size and texture of the fast crack, side tear-lips and hinge bend zones. It was found that the size and texture of these zones varied greatly with impact velocity and specimen temperature. Figure 3 shows scanning electron-micrographs of parts of the initiation, fast crack, side tear-lips and hinge-bend zone to highlight their texture variations. To help in the study and analysis of crack and other failure processes in materials evaluated, high-speed photograpy was used. Two photographic studies (see figures 4(a) and 4(b)) were made to observe crack propagation, one being for a specimen tested at room temperature at an impact velocity of 5 m s^{-1} without side-grooves and the other for a specimen with side-grooves. In the former case, of course, what is seen is the well-rounded cleavage point of the tear-lip following on behind the hidden fast crack in the core of the specimen. Comparing the two photographic sequences, without and with side-grooves,provides useful information on the effect of tear-lips in the specimen.

ANALYSIS

Based on the following equations K_c and G_c were determined using the outputs from sensors in different positions on the specimen and the sensor in the striker.

The specimens had a S/W=4 so $K_c = (6P_c Ya^{1/2})/(BW)$ where P_c is the peak load at crack initiation, a is the length of the sharp pre-crack, B is the thickness and W is the width of the specimen. From LEFM analysis, $G_c = U_c/(BW\phi)$ where U_c is the stored elastic strain energy in the specimen at crack initiation. Table 1 shows a comparison of K_c and G_c values determined from outputs from the two on-specimen sensors and the striker sensor. Values of K_c and G_c calculated using the striker sensor output are greater than if on-specimen sensor outputs are used and this is more so the higher the impact velocity. The point being that the striker sensor monitors the forces acting on the specimen as a whole from the striker not only to initiate fracture but also to generate dynamic vibrations and to impart kinetic energy to the fractured specimen parts. For some calculations and use of derived values, it is also important to take into account the different sizes of the crack initiation, side-lip tearing and hinge-bend section.

TABLE 1 - Examples of K_c and G_c calculations

Impact velocity ($m\ s^{-1}$)	K_c^{st} ($MPa\ m^{1/2}$)	K_c^{sp} ($MPa\ m^{1/2}$)	G_c^{st} ($kJ\ m^{-2}$)	G_c^{sp} ($kJ\ m^{-2}$)
2	2.3	2.1(W/2xW/2) 2.1(W/2xW/8)	3.8	2.7(W/2xW/2) 2.6(W/2xW/8)
5	2.8	2.1 (W/2xW/2) 2.2 (W/2xW/8)	4.6	2.0(W/2xW/2) 2.1(W/2xW/8)
5 (side-grooved)	2.8	2.1(W/2xW/2) 1.9(W/2xW/2)	4.5	1.9(W/2xW/2) 1.7(W/2xW/2)

K_c^{st} and G_c^{st} relate to the sensor on the striker and K_c^{sp} and G_c^{sp} relate to the sensors on the specimen in the W/2xW/2 and W/2xW/8 positions.

CONCLUSIONS

As polymers and their composites are employed in more demanding working conditions so there is a greater need for on-specimen sensors to monitor crack generation and propagation at prepared sites in what can be products of complex shapes. The work presented in this paper as well as providing needed information about the stress distribution in standard three-point bend test specimens subject to high impact velocities has also provided needed information as to the best location for sensors on specimens of various shapes.

ACKNOWLEDGEMENTS

The authors would like to thank Professor J G Williams for his interest and helpful discussion on this work and one of us (JPD) would very much like to thank the interest and support of BP Chemicals Ltd.

REFERENCES

(1) J. G.Williams, "Fracture Mechanics of Polymers" , Ellis Horwood (1984).

(2) J. P. Dear and J. H. MacGillivray, J. Mat. Sci., In Press.

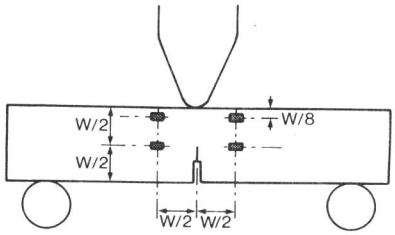

Figure 1 Schematic diagram showing location sites of on-specimen gauges.

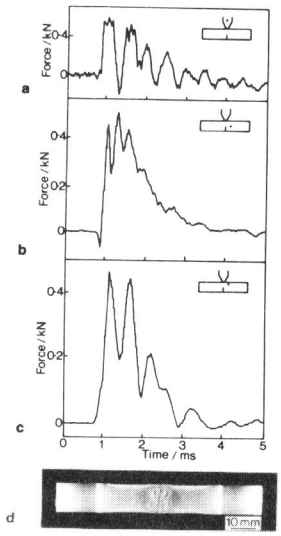

Figure 2 (a)Striker sensor(b)W/2xW/2 sensor(c)W/2xW/8(d) Crack surface.

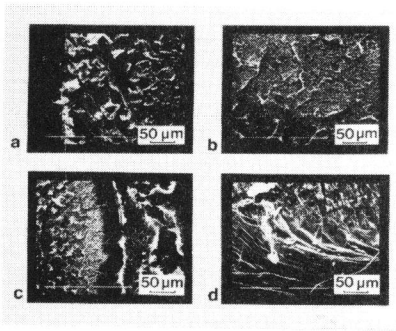

Figure 3 (a)initiation zone(b)fast crack (c)hinge-failure(d)tear-lip.

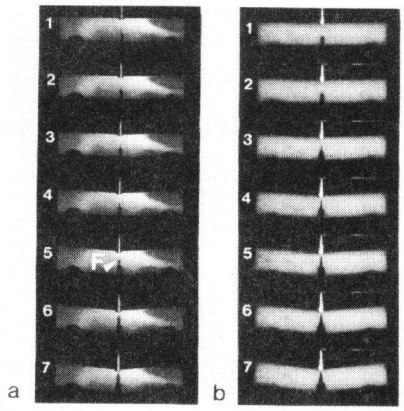

Figure 4 (a) without sidegrooves (b)with sidegrooves.